# The impact of multi-decadal changes in VOCs speciation on urban ozone chemistry: A case study in Birmingham, United Kingdom.

Jianghao Li[1,2], Alastair C. Lewis[1,3], Jim R. Hopkins[1,3], Stephen J. Andrews[1,3], Tim Murrells[4], Neil Passant[4], Ben Richmond[4], Siqi Hou[5], William J. Bloss[5], Roy M. Harrison[5,6], Zongbo Shi[5].

[1]Wolfson Atmospheric Chemistry Laboratories, University of York, York YO10 5DD, UK

[2]School of Water and Environment, Chang'an University, Xi'an 710064, China

[3]National Centre for Atmospheric Science, University of York, Heslington, York YO10 5DD, UK

[4]Ricardo Energy and Environment Gemini Building, Fermi Avenue, Harwell, Oxon OX11 0QR, UK

[5]School of Geography, Earth and Environmental Sciences, University of Birmingham, Edgbaston, Birmingham B15 2TT, UK

[6]Department of Environmental Sciences, Faculty of Meteorology, Environment and Arid Land Agriculture, King Abdulaziz University, P.O. Box 80208, Jeddah 21589, Saudi Arabia

*Correspondence to:* Jianghao Li (cfm531@york.ac.uk)

**Abstract** Anthropogenic non-methane volatile organic compounds (VOCs) in the United Kingdom have been substantially reduced since 1990, in part attributed to controls on evaporative and vehicle tailpipe emissions. Over time other sources with a different speciation, for example alcohols from solvent use and industry processes, have grown in both relative importance and in some cases in absolute terms. The impact of this change in speciation and the resulting photochemical reactivities of VOCs are evaluated using a photochemical box model constrained by observational data during a summertime ozone event (Birmingham, UK), and apportionment of sources based on the UK National Atmospheric Emission Inventory (NAEI) data over the period 1990-2019. Despite road transport sources representing only 3.3% of UK VOC emissions in 2019, it continued as the sector with the largest influence on local $O_3$ production rate ($P(O_3)$). Under case study conditions, the 96% reduction in road transport VOC emissions that has been achieved between 1990 – 2019 has likely reduced daytime $P(O_3)$ by ~1.67 ppbv h$^{-1}$. Further abatement of fuel fugitive emissions was modeled to have had less impact on $P(O_3)$ reduction than abatement of VOCs from industrial processes and solvent use. The long-term trend of increased emissions of ethanol and methanol have somewhat weakened the benefits of reducing road transport emissions, increasing $P(O_3)$ by ~0.19 ppbv h$^{-1}$ in

30 the case study. Abatement of VOC emissions from multiple sources has been a notable technical

31 and policy success in the UK but some future benefits (from an ozone perspective) of the phase out

32 of internal combustion engine passenger cars may be offset if domestic and commercial solvent use

33 of VOCs were to continue to increase.

34

## 1. Introduction

36     Elevated tropospheric ozone ($O_3$) has been a long-standing pollutant of concern in the rural

37 and sub-urban environment and is now becoming more prevalent in urban centers as primary NO

38 traffic emissions reduce (Sicard, 2021). As an important tropospheric oxidant and greenhouse gas

39 (Kumar et al., 2021), exposure to $O_3$ also increases risks of mortality from respiratory diseases and

40 adversely impacts on crop productivity (Lefohn et al., 2018). $O_3$ is mainly formed through

41 photochemical reactions involving the oxidation of volatile organic compounds (VOCs) in the

42 presence of nitrogen oxides ($NO_x$, $NO_x=NO+NO_2$) (Calvert et al., 2015). The release of VOCs arises

43 from a wide range of activities, including unburned fuel or partially combusted products in exhaust,

44 from solvents used in industry and numerous other diffuse domestic and commercial sources (He et

45 al., 2019). Effective policies to mitigate ozone pollution rely on an accurate estimate of both

46 emissions and speciation of $O_3$ precursors.

47     The challenge in reducing $O_3$ lies in its non-linear relationship with its precursors since

48 individual VOCs have unique capacities for forming ozone. Decades of modelling studies have

49 established regimes where reductions in $NO_x$ or VOCs emissions would be preferentially beneficial

50 to mitigate $O_3$ – so-called $NO_x$-limited or VOC-limited regimes (Seinfeld and Pandis, 2016).

51 Abatement of VOCs sources is important in VOCs-limited areas since decreasing the emissions can

52 effectively reduce the local $O_3$ production rate and help limit $O_3$ peak concentrations (Gaudel et al.,

53 2020). The wide range of sources, including many that are diffuse and occur indoors, and differing

54 photochemical reactivities further complicates $O_3$ reduction strategies. Different mixes of sources

55 and speciation can lead to a need for localized policies. For example, short-chain alkanes and

56 alkenes with high hydroxyl radical reactivity emitted from on-road transportation in China, have

57 been reported as being responsible for 26% of national $O_3$ formation (Wu and Xie, 2017). A field

58 observation study in Delhi, India reported that the $O_3$ production in that city was most sensitive to

monoaromatics, followed by monoterpenes and alkenes during a post-monsoon period in 2018

(Nelson et al., 2021). Another study at urban sites in Seoul, South Korea concluded that the $O_3$

production was controlled by C>6 aromatics and isoprene during a summer $O_3$ episode in 2016

(Schroeder et al., 2020). There is therefore no 'one size fits-all' policy in terms for which sources

and sectors to target for optimal $O_3$ abatement efforts.

Policy and regulation aimed at improving air quality in many countries including the United

States, the United Kingdom and Europe have led to decades of falling VOCs emissions (Lewis et

al., 2020; Coggon et al., 2021). This reduction can be substantially attributed to the successful

technical implementation of tailpipe exhaust after-treatment technology for gasoline vehicles

controls on evaporative emissions from vehicles including during re-fueling and a more widespread

set of efforts to control industrial emissions (Winkler et al., 2018). Despite these successes, $O_3$

remains a pollutant of concern; whilst peak concentrations during $O_3$ events have reduced in the UK,

increases in the long-term urban background $O_3$ concentrations have been observed since the 1990s

(Department for Environment, Food & Rural Affairs, 2023). A variety of explanations have been

given to account for the increase including a rising northern hemisphere background $O_3$, increasing

methane which contributes to both global radiative forcing and enhances $O_3$ production (Tarasick et

al., 2019; Abernethy et al., 2021), the increases in non-vehicular sources of VOCs emissions

(Mcdonald et al., 2018; Yeoman and Lewis, 2021), and the reduction of $NO_x$ in VOCs-limited urban

areas leading to greater $O_3$ production efficiency (Sicard et al., 2020).

The UK National Atmospheric Emissions Inventory (NAEI) for VOCs has shown increases in

the relative contribution of solvent usage and the food & wine industry to total national VOCs

emission over 1990-2019, and steady growth in the relative importance of OVOCs within the overall

speciation (Lewis et al., 2020). In North America and Europe cities, OVOCs emitted from volatile

chemical products (VCP) can outweigh fossil fuel sources for urban VOCs. Modelling results

showed that the additional OVOCs from VCP emissions were the most important species for urban

$O_3$ production, increasing the daily maximum $O_3$ mixing ratio by as much as 10 ppbv in Los Angeles

(Qin et al., 2021). Substantial OVOCs emissions can come from unexpected places. For example,

alcohols emitted from use of windshield fluid are now estimated to be a larger VOC source from

road transport than VOC from the tailpipe in the UK (Cliff et al., 2023). From the perspective of $O_3$

pollution, the benefit of substantial reductions on vehicle emissions, whilst there has been a parallel

89    increasing role for non-industrial solvent usage remains unclear. What effect this shift in speciation

90    is having on ozone chemistry is less well studied. One challenge has been the lack of routine

91    measurement of OVOCs in most national air quality monitoring networks (Air Quality Expert

92    Group, 2020).

93        Recent model analysis of decadal trends of ozone has centred on the association between

94    extreme weather and ozone events and projected changes in ozone concentration under chemical

95    regime change scenarios. Significant decline in the UK experiencing ozone episodes and increase

96    in the background ozone concentration are found over the past three decades (Diaz et al., 2020).

97    Elevated ozone mostly occurs in the late spring and summer during anticyclonic conditions when

98    slow moving air masses from continental Europe contribute to accumulation of precursor emissions

99    and enhance photochemical production of ozone (Hertig et al., 2020; Lewis et al., 2021). Higher

100    temperatures in the late summer increase biogenic VOC emissions and reduce ozone deposition,

101    leading to summertime maximum concentrations (Finch and Palmer, 2020). Several studies pointed

102    out that increasingly hot summer due to climate change may offset gains made in the reduction of

103    ozone event over time (Gouldsbrough et al., 2022; Liu et al., 2022). In term of ozone production

104    sensitivity, reductions in NO emissions have led to decreasing trend in annual average concentration.

105    However, 20% or 40% $NO_x$ emission reductions would lead to increases in average and maximum

106    ozone concentrations in the UK with respect to 2018 (Gouldsbrough et al., 2024). In addition to

107    results on $NO_x$ and VOCs sensitivities, Ivatt et al. (2022) revealed that ozone concentrations in North

108    America and Europe were inhibited by aerosol in the 1970s, and this 'aerosol-inhibited regime' has

109    been shifted to Asia by 2014.

110        There have been several recent studies focussed on evaluating the impacts of reductions in

111    anthropogenic sources on ozone production. By integrating the U.S. fuel-based inventory of vehicle

112    emissions (FIVE) into air quality model, McDonald et al. (2018) assessed ozone sensitivity to

113    mobile source $NO_x$ emissions over the Eastern U.S., and Coggon et al. (2021) employed FIVE with

114    volatile chemical products (VCPs) to evaluate contributions of VOC from fossil fuel and different

115    types of VCP emissions to ozone production at an urban background site in New York City. Nelson

116    et al. (2021) used emission inventories from Emission Database for Global Atmospheric Research

117    (EDGAR) to investigate *in -situ* ozone production sensitivity to five inventory source sectors at an

118    urban site in Delhi. Kang et al. (2022) applied two emission inventories in air quality model to

119  evaluate contributions of industry, road transport, power plant, and biogenic emissions to ozone

120  production in Chinese cities. Although great efforts have been made toward identifying crucial VOC

121  sources in regional ozone production, understandings of their roles in urban ozone chemistry in the

122  context of historical changes is still lacking.

123  In this study we evaluate the effects of changing speciation on urban ozone chemistry, using

124  recent field measurements of $O_3$ and its key precursors such as $NO_x$, CO, speciated VOCs and

125  OVOCs in Birmingham, UK during August 2022. We combine this with changing speciation and

126  relative amounts of VOCs based on long-trends in the NAEI. The sensitivity of *in- situ* production

127  and OH reactivities of the measured $O_3$ precursors are investigated by constraining the observational

128  data sets to a zero-dimensional chemical box model. By incorporating the detailed NAEI VOCs

129  emission inventories over the period of 1990-2019 into the model, $O_3$ formation in Birmingham is

130  used as a case study to quantify the impacts of the real-world changes in VOCs sources on urban $O_3$

131  production rate. The relative importance of different VOCs functional group classes to $O_3$

132  production are also evaluated. The results help understand impacts of decades of abating different

133  VOCs-emitting sectors on urban $O_3$ production, and outline the implications for future $O_3$ control

134  strategies.

135

## 2. Materials and Methods

137  2.1 Field observations

138  The observations are taken from the Birmingham NERC Air Quality Supersite during August

139  2022. This is located on the University of Birmingham (52°27'20.2"N 1°55'44.3"W) campus. The

140  site has been in operation for many years, and represents an urban background environment. It is

141  influenced by transport emissions from nearby arterial roads and residential emissions from

142  surrounding area. There are no significant industrial activities within a 4km radius of the site.

143  Continuous measurements of NO, $NO_2$, CO, $CH_4$, VOCs, $O_3$, along with meteorological

144  parameters including air temperature and pressure, relative humidity, wind speed and direction were

145  made. Briefly, NO and $NO_2$ were measured by a chemiluminescence-based T200 analyzer (Teledyne

146  API., U.S.A.) and the T500U Cavity Attenuated Phase Shift (CAPS) analyzer (Teledyne API.,

147  U.S.A.). The concentration of $NO_x$ was then the statistical sum of NO and $NO_2$. The mixing ratio of

148 CO were measured by a laser absorption spectroscopy Multi-species Continuous Emissions

149 Monitoring instrument (Enviro Technology Service Ltd., UK) (Li et al., 2020). Manual calibration

150 and span checks for the above instruments were performed every 3 days, and automatic zero

151 calibration was set on daily bases. $O_3$ was measured by an $O_3$ analyzer (Model 49i, Thermo Fisher

152 Scientific Inc., U.S.A.) with a minimum detection limit (MDL) of 1.0 ppbv. Meteorological

153 parameters including air temperature and pressure, and relative humidity were obtained from a

154 weather station WS300-UMB weather station (Luff GmbH, Germany). Additionally, Wind speed

155 and direction were measured by a 3-axis ultrasonic anemometer (Gill Instruments Ltd., UK) over

156 the campaign.

157 A gas chromatography-flame ionization detection (GC-FID) analysis system (7890A, Agilent

158 Technologies, U.S.A.) was used to quantify 38 individual VOCs species. Details on instrument

159 settings and quality assurance/quality control methods can be found in (Warburton et al., 2023).

160 Briefly, the GC-FID system utilizes dual detectors: one detector for $C_2 - C_6$ non-methane

161 hydrocarbons (NMHCs)；the other detector for remaining $C \geq 7$ hydrocarbons, and polar species

162 such as ethers, ketones, and alcohols. Ambient samples were dried at $-40$ °C using a water trap and

163 then preconcentrated on a carbon adsorbent at the lowest temperature the unit could achieve, always

164 lower than -115 °C. Once a 0.5L sample had been collected, a pre-concentration trap was warmed

165 slightly from -80 °C to purge trapped atmospheric $CO_2$. The trap was then heated to 190 °C for 3

166 minutes with a counter flow of helium thermally desorbing the concentrated VOCs onto focusing

167 micro-trap held at lower than -115 °C. The analytes were flash heated and passed onto a VF-WAX

168 column. The unresolved analytes ($C_2 - C_6$ NMHCs) were then transferred into a $Na_2SO_4$-deactivated

169 $Al_2O_3$ porous-layer open tubular (PLOT) column via a Deans switch, for separation and detection

170 by the first FID. The Dean switch then diverted the analytes onto a fused silica internal diameter to

171 balance column flows and subsequently transfer the VF-WAX column- resolved species into the

172 second FID. Generally, quantification of $C_2$-$C_6$ hydrocarbons was completed by the first FID using

173 4 ppbv gas standard cylinders (the National Physical Laboratory, Teddington, UK). Quantification

174 of $C \geq 7$ hydrocarbons and OVOCs was completed by the second FID using effective carbon number

175 (ECN) with reference to toluene. In this study, the concentration of total VOC (TVOC) was defined

176 as the statistical sum of concentrations of measured individual species, but this is not meant to infer

177 that this represents the total reactive carbon in air, which would always be greater than this value

178 due to unmeasured species. Later in this study we broadly group species according to their chemical

179 function groups, summing into alcohols, ketones, alkanes, alkenes, aromatics, aldehydes, and

180 alkynes.

181 The GC-FID system responses were regularly checked by running direct calibration sequences

182 using the 4 ppbv gas standard cylinders. It was verified there was no FID-response drift over the

183 analyzing period for this study. Additionally, carbon-wise FID responses for all reported species

184 were calculated to verify the use of ECN as a quantification method. Table S1 lists which species

185 were directly calibrated, and which used equivalent carbon numbers for quantification. Table S2

186 shows effective carbon numbers of species which used carbon-wise responses.

187 2.2 National emission inventory for VOCs

188 Estimates of UK anthropogenic VOC emissions are taken from the NAEI. The NAEI uses a

189 combination of UK-specific methods and default methods as recommended in the European

190 Monitoring and Evaluation Programme (EMEP)/European Environment Agency (EEA) Emission

191 Inventory Guidebook (European Environment Agency, 2016). Further details can be found in (NAEI,

192 2021). The VOC inventory is also disaggregated into inventories for each individual VOC species

193 and details of the speciation process and assumptions can be found in (Passant, 2002) and (Lewis et

194 al., 2020).

195 Methods to estimate emissions can be divided into two groups: those using emission factors,

196 and those using 'point source' emissions data reported to regulators by the operators of individual

197 industrial sites. The emission factor methods require UK activity data, for example consumption of

198 paint, consumption of a fuel, production of steel or vehicle kilometers travelled. The activity data is

199 then combined with an emission factor which expresses the total VOC emission that is expected per

200 unit of a given activity. Most total VOC emission factors are taken from the internationally applied

201 EMEP/EEA Emission Inventory Guidebook and so are not necessarily UK-specific. The factors for

202 road transport are directly calculated for the UK and a particularly detailed approach is used to

203 estimate emissions using emission factors from the Guidebook for many different vehicle types and

204 emission standards, fuels and road types combined with detailed transport activity from the UK

205 Department for Transport. Government statistics cannot always provide the necessary activity data

206 for other sectors, so industry data are used instead. For instance, NAEI data on consumption of

207 products containing organic solvents are from industry sources. The alternative point source method

208  can be used for source categories where emissions data can be obtained for all sites within the sector,

209  and this limits the method to source categories such as crude oil refining, steel production and

210  chemicals production. The emissions data reported by the operators of these sites can be based on

211  emissions monitoring, although this is not always the case and emissions might instead be estimated,

212  for example, using emission factors.

213      The NAEI produces updates to the inventory for total VOC mass emissions by source sector

214  each year to achieve a consistent historic time-series reflecting trends in UK emissions. Emissions

215  of individual VOC species are estimated using source-specific speciation profiles which show the

216  mass fraction of each species, or in some cases groups of species, emitted by the source (NAEI,

217  2021; Passant, 2002). Over 600 individual VOC species or species groups are included in the

218  speciation, based on sources in industry, regulators and in some cases literature sources and

219  databases such as the USEPA SPECIATE database. The speciated inventory tends to be more

220  uncertain than the estimation of total mass of VOC emissions. The inventory for total VOC mass is

221  updated annually, whereas the speciation profiles are only periodically updated when new

222  information becomes available. Thus, trends in a particular species for a sector are a reflection of

223  changes in total VOC emissions for the sector and do not normally reflect any changes over time in

224  the speciation profile of the sector which may have occurred.

225  2.3 Photochemical box model

226      The framework for evaluating effects of changing VOCs speciation is a 0-D Atmospheric

227  Modelling chemistry box model (Wolfe et al., 2016), driven by the Version 3.3.1 of the Master

228  Chemical Mechanism (MCM v3.3.1) (Saunders et al., 2003; Jenkin et al., 2003). The model can be

229  effective in identifying the instantaneous *in- situ* $O_3$ sensitivity to changes in individual VOCs. The

230  measured concentrations of 38 VOCs species, $NO_x$, and CO, along with air temperature and pressure,

231  and relative humidity were averaged to a time resolution of 1-hour to constrain the model. A 3-day

232  model spin-up, with each 24-hour model run constrained by the observational data, was performed

233  in order to initialize the unmeasured compounds and transient radicals. The modelled outputs on the

234  4th day were taken as representing steady state of the photochemistry.

235      Photolysis rates were calculated as a function of solar zenith angle (Saunders et al., 2003):

236  $$J = l(\cos \chi)^m \exp(-n \sec \chi) \tag{1}$$

237  Where *J* is the photolysis rate in s[-1]; *l*, *m*, *n* are constants derived from radiative transfer model

238 runs for clear sky condition at an altitude of 0.5 km and literature cross sections/quantum yields; $\chi$

239 is the solar zenith angle in radians.

240     The net production rate of $O_3$ ($P(O_3)$) is calculated by the difference of the production rate of

241 $O_3$ and the destruction rate of $O_3$, as in Equation (2):

$$
\begin{aligned}
P(O_3) = &(k_{HO_2+NO}[HO_2][NO] + \sum_i k_{RO_{2_i}+NO}[RO_2][NO]) - \\
&(k_{O^1D+H_2O}[O^1D][H_2O] + k_{O_3+OH}[O_3][OH] + k_{O_3+HO_2}[O_3][HO_2] \\
&k_{NO_2+OH}[NO_2][OH] + \sum_i k_{RO_{2_i}+NO_2}[RO_2][NO_2])
\end{aligned} \tag{2}
$$

243     Where the former part is the rate of $O_3$ production, representing by rate of NO oxidation by

244 $HO_2$ and $RO_2$ radicals; the latter part is the destruction rate of $O_3$, calculating by the sum of the rate

245 of $O_3$ photolysis, the rates of the reactions with OH and $HO_2$ radicals, and the rates of $NO_2$ loss

246 through reactions with OH and $RO_2$ radicals.

247     The sensitivity of $O_3$ to its precursors is quantified by the index of relative incremental

248 reactivity (RIR) (Liu et al., 2022b), as in Equation (3):

$$
RIR = \frac{\Delta P(O_3)}{P(O_3)} \times a^{-1} \tag{3}
$$

250     Where RIR is the Relative Incremental Reactivity in %/%, $\Delta P(O_3)/P(O_3)$ is the ratio of the

251 change in $O_3$ production rate to the base $O_3$ production rate; $a$ is the reduction percentage in the

252 input concentration of $O_3$ precursors – a factor that allows for the effects of changing absolute

253 amounts of VOCs to be evaluated. Here a value of 30% was adopted for $a$.

254

## 3. Results and Discussion

256 3.1 Observation overview

257     The time series of $O_3$ and its precursors during August 2022 are shown in Figure 1, subdivided

258 into periods that will be referred to as 'initial period', '$O_3$ period', and 'clear–out'. The three periods

259 covered 1st August-21th August 2022. Each period included one full week to avoid

260 weekday/weekend differences in $NO_x$ and VOCs concentrations impacting differently when $O_3$

261 production was compared between the three periods (de Foy et al., 2020). Ozone showed a generally

262 increasing trend from 1st to 14th August and then returned to relatively low concentrations after 15th

263 August 2022. The daily maximum 8 h average $O_3$ concentrations (MDA8h $O_3$) during the $O_3$ period

264 exceeded the WHO guideline value (100 $\mu g\ m^{-3}$), ranging from 111 to 153 $\mu g\ m^{-3}$. The elevated $O_3$

265  during the middle of the month corresponded to more intense photochemical formation under hot

266  weather conditions (32.7 ℃ in maximum) and higher concentrations of $O_3$ precursors (Table S3).

267  The diurnal profile of NO and $NO_2$ in the three periods generally showed a bimodal pattern,

268  albeit less pronounced in the initial and clear–out periods (Figure 2). The two peaks likely arise as

269  a consequence of increased traffic volumes at the start and end of the day, coupled to boundary layer

270  height changes in the early morning and into the evening (Lee et al., 2020). The average

271  concentrations of $NO_2$ during 05:00-10:00 were 10.8 ppbv in the $O_3$ period, which was considerably

272  higher than the concentration of 3.9 ppbv in the initial period and 3.4 ppbv in the clear–out period.

273  The low level of NO in the $O_3$ period highlights the rapid consumption of NO via photochemical

274  processes. The oxidation of CO is an important source of $HO_2$ in the atmosphere (Chen et al., 2020),

275  here in the range of 82.5 to 134.2 ppbv with little difference between periods. The diurnal profiles

276  of $O_3$ peaked at 15:00, with maximum hourly concentrations of 31.6, 67.2, and 30.4 ppbv in the

277  initial, $O_3$, and clear–out periods, respectively. Slight decreases in $O_3$ were observed during

278  nighttime (00:00-05:00), indicating enhanced NO titration effects.

279  The detailed VOCs composition in the three periods is presented in Figure S1. Concentration

280  of TVOC were 19.4 ± 8.4, 48.0 ± 18.8, and 23.5 ± 12.5 μg m$^{-3}$ in the three periods, respectively.

281  Alcohols, represented mainly by methanol and ethanol, were the predominant group that contributed

282  40.3% - 47.4% of over measured VOCs mass. This was followed by alkanes (21.4%-24.6%) and

283  ketones (16.3%-17.3%). Contributions of aldehyde (acetaldehyde), aromatics, alkenes, and

284  acetylene were low, ranging from 1.0% to 9.4% of total mass. Average mixing ratio of the top 10

285  species in selected periods at Birmingham Supersite are listed in Table S4. The top 10 species were

286  represented by methanol, acetone, ethanol, acetaldehyde, and $C_2 – C_4$ alkanes across initial period,

287  $O_3$ period, and clear-out period. The top individual species contributing to the total VOCs were

288  methanol (10.3% – 33.6%) and acetone (15.5% – 17.1%), regardless of the subdivided periods. The

289  results highlight large emissions of ethane, propane, n-butane, and i-butane associated with Natural

290  Gas (NG), Liquefied Petroleum Gas (LPG), and propellant use, fuel combustion and evaporation.

291  Ambient VOCs largely influenced by combustion-related sources (i.e., vehicle exhaust and coal

292  combustion) generally show alkane-dominated composition (Wu and Xie, 2017). Here, the

293  composition and amount of VOCs observed were most likely influenced by non-combustion

294  processes such as volatile chemical product usage and industrial processes (Gkatzelis et al., 2021).

Methanol was the most abundant VOC with an average concentration of 4.1 ppbv, followed by acetone (2.0 ppbv), ethane (1.9 ppbv), ethanol (1.8 ppbv), and acetaldehyde (1.0 ppbv). The average ratio of ethene/ethane was $0.2 \pm 0.1$ over the campaign, considerably lower than seen in polluted locations, e.g. Hong Kong (China) ($0.7 \pm 0.1$) (Wang et al., 2018) and Seremban (Malaysia) (1.1) (Zulkifli et al., 2022).
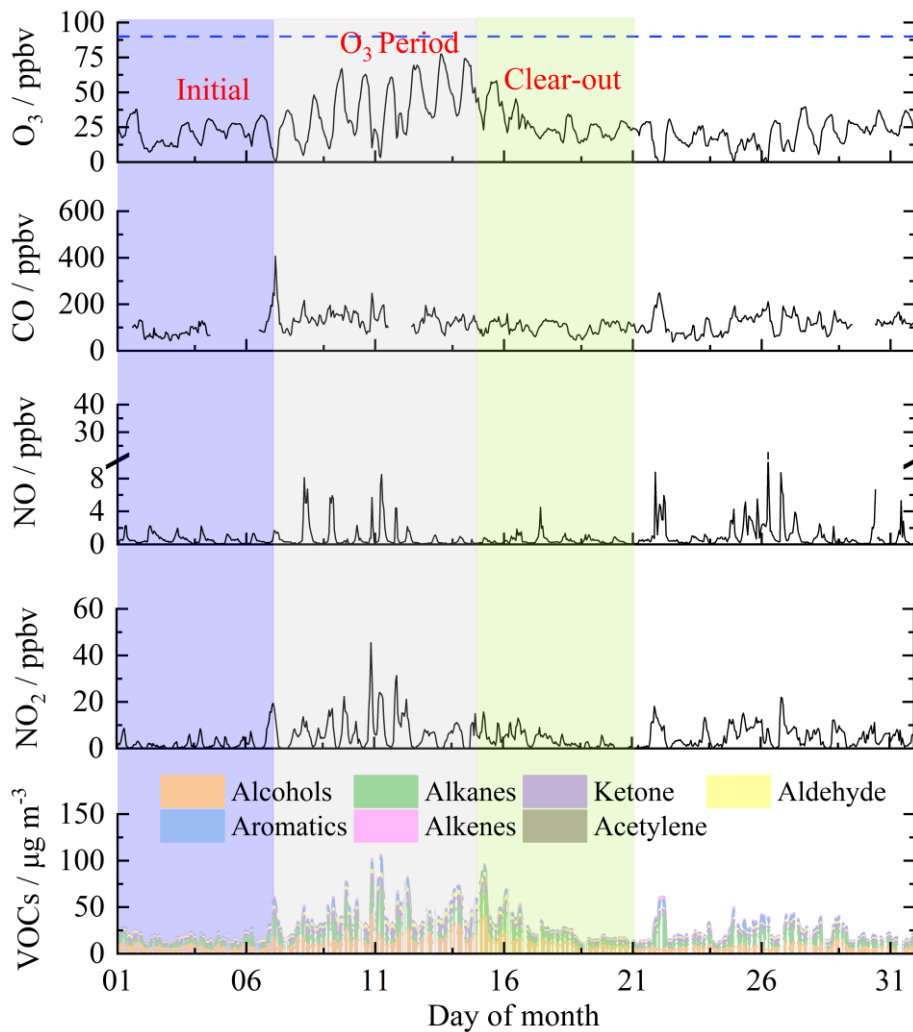


Figure 1. Time series of $O_3$, CO, NO, $NO_2$, and VOCs groups at the Birmingham Supersite. The blue dash line denotes the national standard (90 ppbv) for hourly $O_3$ concentration.
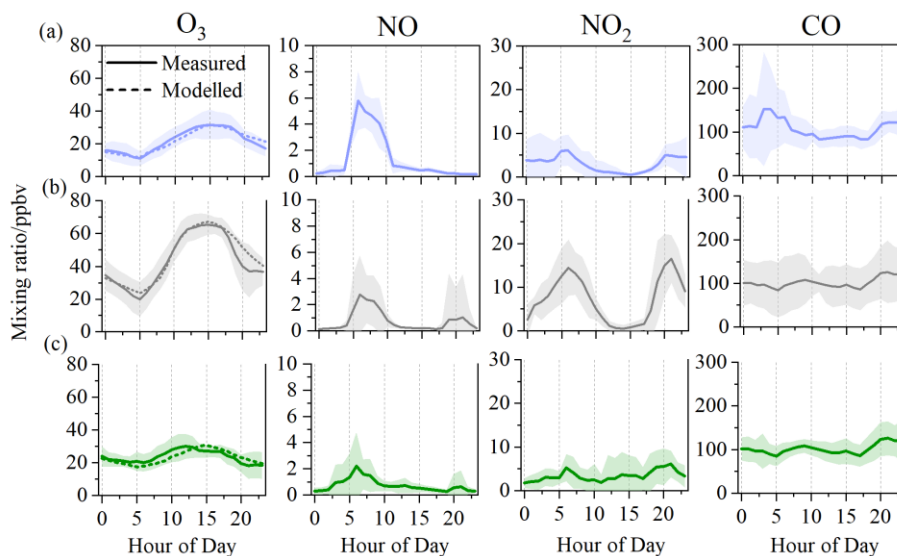
Figure 2. Diurnal variations of $O_3$, NO, $NO_2$, and CO during the initial (a), $O_3$ period (b), and clear–out period (c). The shaded areas represent standard variations.

The general diel profiles for all selected VOCs, except for ethane, showed bimodal pattern (Figure S2). Concentrations were much higher during the night, and lower in the day, due to they were subject to photochemical losses during the daytime. The bimodal pattern is less apparent for methanol and acetone, as they are abundant species originating from many anthropogenic sources in urban areas. For example, methanol was the most abundant species measured at a roadside in UK using Thermal Desorption-Gas Chromatography coupled with Flame Ionization Detection (TD-GC-FID) (Cliff et al., 2023). A separate study on gasoline and diesel vehicle exhausts reported methanol and acetone were the largest OVOCs emitted (Wang et al., 2022). Gkatzelis et al. (2021) conducted Positive Matrix factorization (PMF) analysis based on observed VOCs dataset in New York City, and concluded that acetone was the second most abundant species in measurements and was mostly attributed to volatile consumer product emissions (90%). (See Section 3.3 for further discussions for anthropogenic sources of OVOCs).

3.2 Observation-based $O_3$ formation sensitivity

The *in -situ* $O_3$ formation sensitivity was examined via reaction rates of ozone precursors and OH radical (OH reactivities, ($k$(OH))) and RIR scales of ozone precursors, along with the chemical budgets of $O_3$ formation and loss. In initial and clear-out periods. $k$(OH) exhibited consistent diurnal patterns, ranging from 2.4 to 5.9 $s^{-1}$ (Figure S3). In the $O_3$ period, $k$(OH) reached 9.0 and 8.7 $s^{-1}$ at approximately 07:00 and 20:00, respectively. A rapid increase in $k$(OH) was observed in the early

326    morning (00:00-06:00). VOCs and model generated species represented 60.5%, 65.7%, and 56.7%

327    of the total $k$(OH) in the three periods, respectively. $NO_x$ and CO only contributed 10.2% -27.9% to

328    total $k$(OH). Among of the VOCs groups, alcohols exhibited the largest $k$(OH) in all periods,

329    accounting for 5.0% - 6.9% of the total $k$(OH). The diurnal production and loss of $O_3$ are shown in

330    Figure S4. The oxidation and photolysis of VOCs promoted the production of $RO_2$, and $NO+RO_2$

331    contributed 47.7% of the $O_3$ production pathways in the $O_3$ period and 36.2% and 39.8% in initial

332    and clear–out periods, respectively. Considering $O_3$ destruction, $OH+NO_2$ was the most important

333    pathway during morning (08:00-12:00), accounting for 73.5%, 55.4% and 59.4% of the $O_3$

334    destruction pathways in the three periods. The dominant $OH+NO_2$ contribution to $O_3$ destruction

335    suggested that the *in -situ* $O_3$ productions in all three periods was sensitive to VOCs emissions to

336    some extent.

337        In order to understand contributions of $O_3$ formation from direct emissions and secondary

338    formations of OVOCs, we developed two modelling scenarios: (1) all OVOCs species were

339    constrained to observed mixing ratio; (2) all OVOCs species were unconstrained. (2) allowed

340    secondary formations of OVOCs by oxidations of their precursor VOCs. As shown in Figure S5,

341    secondary formations of OVOCs had little impact on $O_3$ formation in all periods. The simulation of

342    $O_3$ production using the box model without constraining observed OVOCs slightly underestimated

343    average daily maximum $O_3$ mixing ratio and P($O_3$), compared to the scenario with all observed

344    OVOCs species constrained. The underestimation for average daily maximum mixing ratio of $O_3$

345    was 4.8%, 6.9%, and 5.1% in initial period, $O_3$ period, and clear-out period, respectively. In this

346    case, the underestimation of average daily maximum P($O_3$) was 5.1%, 6.0%, and 9.3% in the three

347    periods, respectively. The results demonstrated that in the Birmingham case study, primary

348    emissions of OVOCs played central role in the *in -situ* ozone production.

349        The relative incremental reactivity of $NO_x$, CO, and anthropogenic VOCs (AVOCs, all

350    measured VOCs except for isoprene) are shown in Figure 3. The *in -situ* $O_3$ production was most

351    sensitive to anthropogenic VOCs with the highest positive RIR values (0.44 - 0.49). This is as

352    anticipated given earlier analyses demonstrating their role in determining $k$(OH) and $O_3$ production.

353    The low RIR (0.03 - 0.07) for CO in all three periods indicated a minor contribution of CO oxidation

354    to $O_3$ production. The high RIR (0.24) for $NO_x$ was only observed in the $O_3$ period. Acetaldehyde

355    showed the highest positive RIR (0.17 - 0.19) among the AVOCs, suggesting that the photolysis and

356    oxidation of acetaldehyde was a limiting factor for $O_3$ formation. The important role of carbonyl

357    compounds in atmospheric photochemistry has also been reported in previous studies, contributing

358    up to 59.3% to the $O_3$ formation in ambient environments in China, the United States, and Brazil

359    (Qin et al., 2021; Liu et al., 2022a; Edwards et al., 2014). Alkanes and alcohols exhibited lower RIR

360    values (0.02 - 0.04), despite their high mass concentrations.
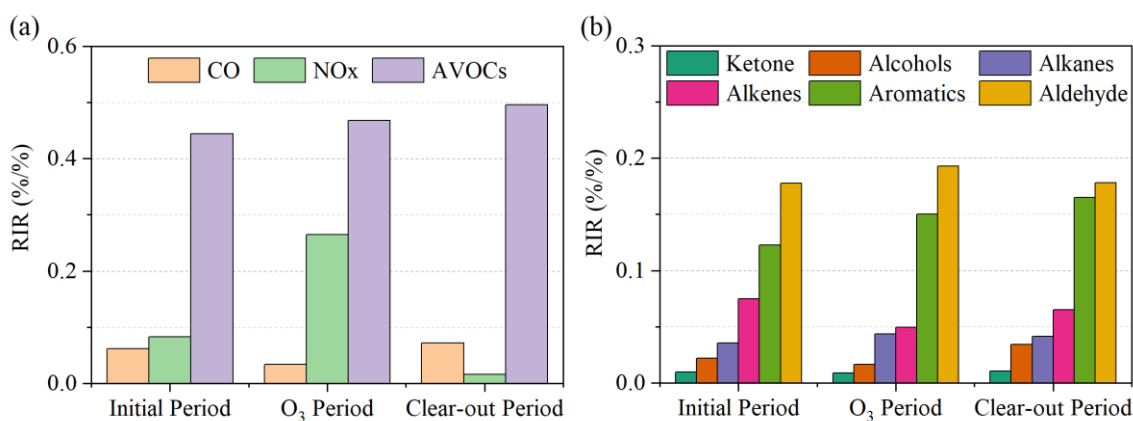


361

362    Figure 3. Modelled RIRs for (a) major $O_3$ precursors and (b) the AVOCs groups during

363    photochemically active daytime (08:00-16:00) in the selected periods. (AVOCs: anthropogenic

364    VOCs, all measured VOCs except for isoprene)

365

366    3.3 Emission inventory-informed $O_3$ production sensitivity tests

367      The trends in anthropogenic VOCs emissions from 1990 to 2019 estimated by the NAEI are

368    shown in Figure S6. Over the period, the annual national emissions decreased by ~69.0% from 2,941

369    kt in 1990 to 911kt in 2019. The reduction is partly attributed to more stringent controls for gasoline

370    vehicle emissions, both tailpipe and evaporative/fugitive. In 2019, VOCs emissions from on-road

371    transport and fuel fugitive losses accounted for only 3.3% and 13.7% of the total mass of VOCs

372    emissions, compared to 29.1% and 26.9% in 1990. Efforts have also been directed towards

373    controlling industrial processes, commercial solvent usage, and combustion emissions, resulting in

374    reductions of 66.8%, 48.9%, and 20.7%, respectively over the period. However, contributions from

375    solvent usage to total VOCs emissions over 1990-2019 showed only modest reductions in the 1990s

376    and 2000s and indeed small increases in the most recent years (Figure 4(b)). This slight growth in

377    solvent usage is due to increasing emissions from solvent use in consumer products such as

378    decorative products, aerosols, personal-care products, and detergents (NAEI, 2021). Solvent usage

379    had become the largest contributory sector (33.7%) to VOCs emissions by 2019, followed by

14

380      industrial processes (16.0%).

381         As shown in Figure 4(a), the VOC speciation over the 1990-2019 period was dominated in mass

382      terms by contributions from alkanes and alcohols, the former decreasing as gasoline sources

383      declined, the other increasing as non-industrial solvent and food and drink industry processes

384      emissions followed a different pattern. Alkane emissions fell from 46.6% to 30.6% over the period.

385      Further reductions in alkane emissions are expected from policies for that phase-out sales of new

386      internal combustion engine vehicles in the UK (and in many other places) by 2035. Growth in the

387      relative contributions of alcohols was primarily driven by increases in emissions of methanol and

388      ethanol, and to a lesser extent in 1-butanol and 2-propanol (Figure 4(c)).
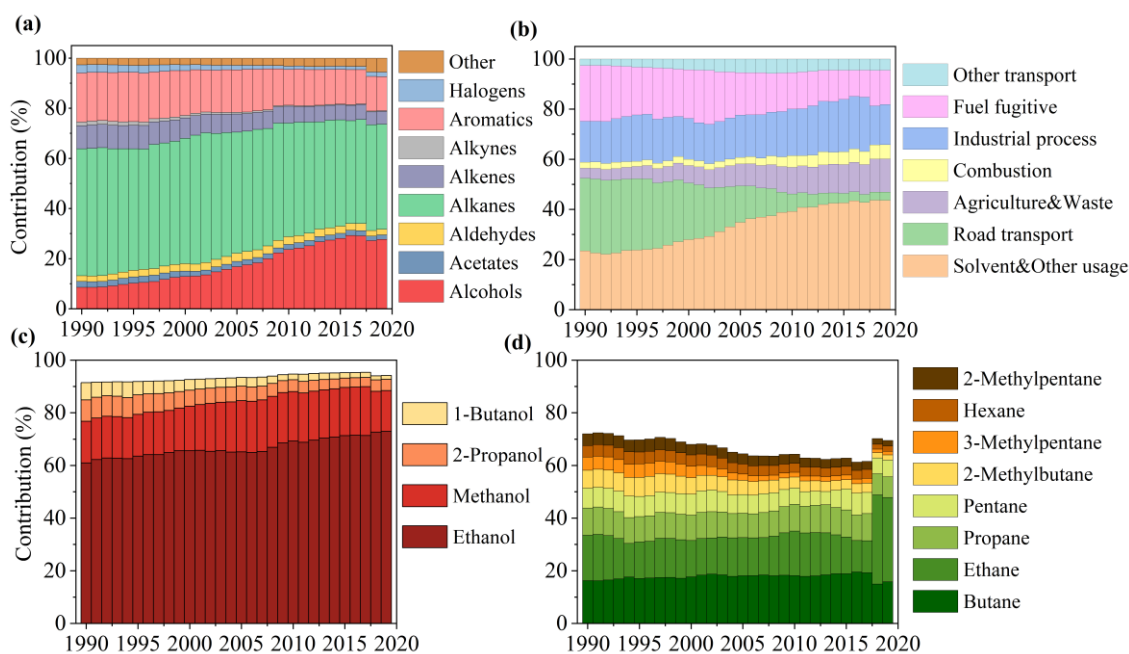


390 Figure 4. Contributions to annual national UK emissions of VOCs between 1990-2019 by: (a)

391 functional group; (b) by major emissions reporting sector; (c) for four individual alcohols in the

392 overall sub-class of alcohols; (d) for eight individual alkanes in the sub-class of all alkanes.

393

394      Figure S7 shows UK emission trends of individual species from different VOCs classes. These

395 highlight a national trend since 1990 of decreasing emissions of ethane associated with natural gas

396 leakage, toluene and propane associated with on-road petrol evaporation, as well as reductions of

397 benzene, ethene, and acetylene associated with tailpipe exhaust. Meanwhile, the reduced emissions

398 have been accompanied with increases in emissions of methanol and ethanol. The increase in

399 methanol is largely attributed to increased emissions from car-care products (i.e., non-aerosol

400  products). The increase in ethanol is due to increased domestic and industrial solvent usage.

401      The $NO_x$, CO, and VOC speciation within the NAEI for each of the six major emission sectors

402  was used to assign proportional sectoral contributions to the VOCs observed in Birmingham, and

403  hence to ozone production in the case study. (Table S5). Isoprene was excluded from the analysis as

404  it is assumed to have an entirely biogenic source. The six sectors are: road transport (both of on-

405  road exhaust emission and evaporative losses of fuel vapor), industrial processes, combustion,

406  solvent usage, fuel fugitive, and agriculture emissions). This makes a key assumption that the VOCs

407  at the observation site are affected directly in the same proportion that VOCs are reported in national

408  amounts in the NAEI. We make this assumption since it provides a reasonable starting point for

409  understanding how each VOC sector may influence $O_3$ production during a case study event,

410  however ozone formation might be sensitive to differing regional distribution in speciation. The

411  attribution of VOCs sources based on the NAEI data can be thought of as representative for this

412  case study as a typical urban environment, but it might not hold for cities near large industrial VOC

413  sources (i.e., oil refinery and industrial production sites), since they can significantly affect

414  composition and chemical reactivity of ambient VOCs.

415      Figure S8 shows the modelled RIRs for these sources in the initial, $O_3$, and clear–out periods.

416  All the sources generally showed higher RIR values in the $O_3$ period. Road transport exhibited the

417  highest positive RIR values in all periods (0.30 - 0.36), followed by industrial process (0.06 - 0.09)

418  and solvent usage (0.05 - 0.07). Despite being a relatively minor contributor to the mass of national

419  VOCs emissions (only 3.3% of the total in 2019), road transport VOCs still played the most

420  important role in local ozone photochemical chemistry, in this case study.

421      Figure 5a shows the changes in $P(O_3)$ during the $O_3$ period from 08:00 to 16:00 which might

422  arise as a result of reductions in the individual sectors described above. For this analysis, emission

423  changes in these sectors can be obtained by reducing model constrained concentrations of VOCs,

424  $NO_x$, and CO according to their contributions arising from individual emission sectors. This is a

425  'thought experiment' where under 2019 general observed atmospheric conditions (e.g., for $NO_x$, CO

426  and so on), each of the VOC source sectors is then further reduced in isolation (from 2019 levels)

427  and the effects on $\Delta P(O_3)$ were evaluated. Based on these scenarios, reducing emissions from the

428  individual sectors all resulted in decreased $P(O_3)$, as would be anticipated. Reducing ozone

429  precursors arising from road transport would lead to a decreased $P(O_3)$ of ~1.71 ppbv $h^{-1}$ if that

sector could be 100% abated in the case study. This is expected because road transport is a source

of photochemically reactive VOCs, including aromatics, aldehyde, and short-chain alkanes/alkenes.

Other sectors showed more modest effects, with reductions in solvent-related VOCs the next most

significant lever to control ozone. Fully abating emissions of all industrial and solvent process

emissions only resulted in a decreased $P(O_3)$ of ~0.35 ppbv $h^{-1}$, largely because they are dominated

by ethanol and methanol with relatively low RIR values. Considering the real-world changes in

VOC emissions over the period of 1990 to 2019, the very major reductions in road transport

emissions have led to the largest effects in reducing $P(O_3)$ (Figure 5(b)). Whilst there have also been

some very large reductions (94.6%) in fuel fugitive emissions, the impact on $P(O_3)$ reduction is

modelled to have been relatively modest, being similar to industrial processes and solvent usage. It

is important to acknowledge the limitation of this analysis. In the real world, reductions in ambient

VOCs from the NAEI sectors are affected by photochemical loss rate and advection processes,

potentially altering the proportion of VOCs that would be observed with each sector reduction at

the measurement site. This would potentially be an important consideration if instantaneously

radical budgets were being evaluated, but it is a less significant issue when integrated ozone

production effects.
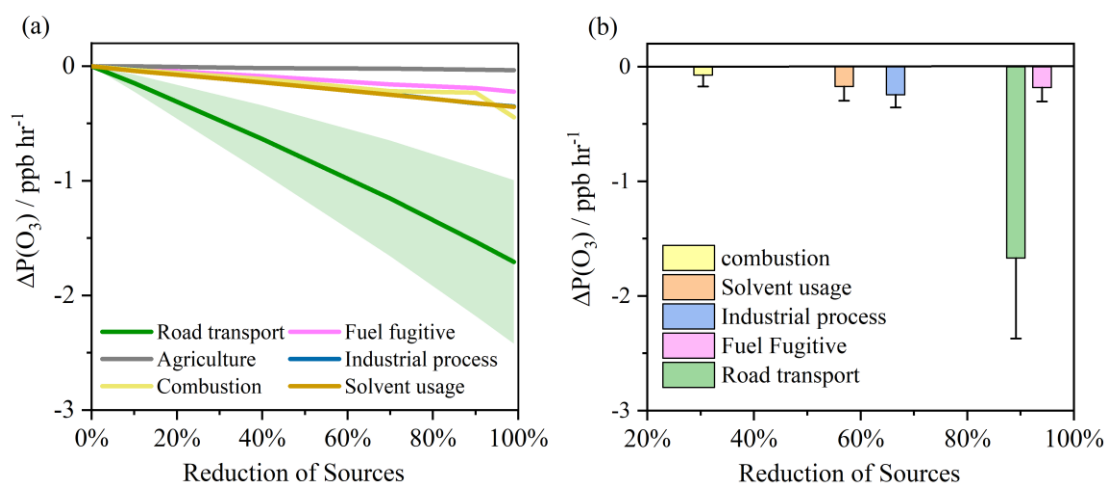


Figure 5. (a) Changes in $P(O_3)$ in response to different reductions in VOCs, $NO_x$, and CO from

different sectors for the Birmingham-case study condition. (b) Changes in $P(O_3)$ based on the NAEI

estimated reductions in VOCs from different sectors between 1990 and 2019. The standard

deviations represent variability in $\Delta P(O_3)$ during 08:00-16:00 LST in the $O_3$ period.

Further model runs were performed to better understand the impacts of the shift between

453    alkanes and alcohol species on $P(O_3)$, given trends showing decreasing alkanes emissions and

454    increasing alcohol emissions between the 1990-2019 period (Figure 4). The modelled alkane

455    concentrations in the case study were reduced by 10%, 30%, 50%, 70%, 90%, and 99%. This

456    represents a downward trajectory in alkane emissions that would be anticipated as gasoline vehicles

457    are slowly retired. Two further scenarios were then developed to sit alongside these reductions in

458    alkanes. Firstly, the concentration of ethanol was increased to keep the overall total VOC

459    concentrations in the model under case study conditions unchanged. Second, the concentration of

460    both ethanol and methanol were scaled upwards to keep total VOCs concentration unchanged. As

461    shown in Figure 6, reductions in alkanes alone resulted in decreased $P(O_3)$ to a maximum of ~0.26

462    ppbv h$^{-1}$ if fully abated. If that alkane reduction was balanced with increased ethanol and methanol,

463    then $\Delta P(O_3)$ is reduced by a maximum of 0.19 ppbv h$^{-1}$. If alkane reductions were balanced by

464    increasing ethanol alone, then $P(O_3)$ still decreases, but only up to 0.07 ppbv h$^{-1}$.
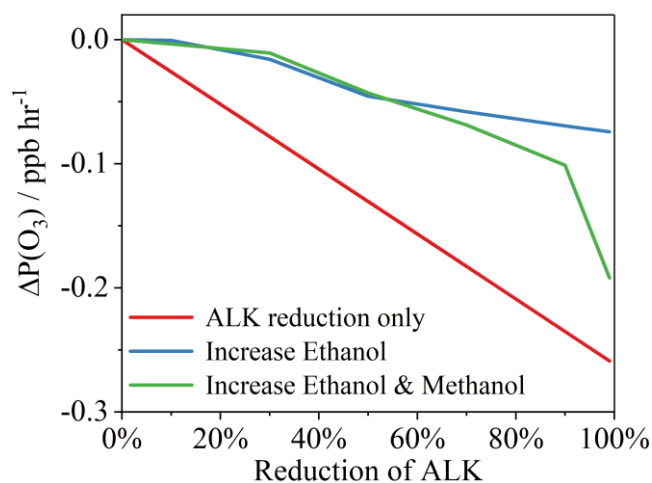


465

466    Figure 6. Reductions in $\Delta P(O_3)$ based on reducing alkanes (ALK) in the model (under case study

467    conditions), reducing alkanes but balancing the overall VOC amount with increased ethanol (blue

468    line) and reducing alkanes but balancing the overall VOC amount with increased ethanol and

469    methanol (green line).

470

## Conclusion

472        In this study a typical high-$O_3$ event in Birmingham, United Kingdom was chosen as a case

473    study to investigate the impacts of changes to VOCs emissions and speciation on urban $O_3$

474    production. The *in- situ* $O_3$ formation sensitivity was split into three periods: initial, high $O_3$, and

475 clear–out. Results from OH reactivity, $O_3$ budgets, and RIR index showed that $O_3$ formation in all

476 three periods was impacted by both VOCs and $NO_x$, but was more sensitive to anthropogenic VOCs.

477 The oxidation of alcohols and photolysis of acetaldehyde substantially contributed to *in- situ* $O_3$

478 formation, especially in the high $O_3$ period. The roles of anthropogenic VOC sources in urban $O_3$

479 chemistry were examined by integrating the NAEI speciation over the period of 1990-2019 into

480 photochemical box model scenarios. Despite road transport only contributing 3.3% of national

481 VOCs emissions in 2019 it still played the most important VOC role in the case study ozone

482 photochemistry, when inventory contributions were mapped onto observed VOCs. Sequentially the

483 observed VOCs were reduced by the fractional contributions and speciation in the NAEI for six

484 sectors to evaluate what impact abating different VOCs-emitting sectors would have on $P(O_3)$.

485 Abating road transport VOCs in isolation would lead to a decreased $P(O_3)$ by up to 1.67 ppbv h$^{-1}$,

486 but abating other sectors such as solvent use and fugitive fuels had noticeably smaller effects.

487 Despite emissions of VOCs from road transport falling very dramatically between 1990 and 2019,

488 it remains one of the most powerful means to further reduce ozone in this typical UK case study.

489 The wider shift in speciation reported in the NAEI from alkanes to alcohols was also examined

490 using scenarios where emission reductions for alkanes, were counterbalanced with increases in

491 alcohols, all simulated for the Birmingham case study conditions (e.g., for $NO_x$, CO and etc). Further

492 reducing alkanes from present day conditions to zero has a clear beneficial effect on reducing $P(O_3)$

493 by up to ~0.26 ppb hr$^{-1}$. However, this benefit would to a degree be offset should alcohol emissions

494 (for example from food and drink, and/or solvent use) increase to counterbalance those alkanes

495 reductions. Whilst simple alcohols are inherently less potent ozone-forming VOCs compared to the

496 mixture of VOCs from road transport, avoiding future growth in emissions remains important, since

497 they weaken the long-term benefits of road transport electrification and the phase out of internal

498 combustion engine vehicles.

499

## Data Availability

501 Observational data including meteorological parameters and air pollutants used in this study are

502 available at https://github.com/nervouslee/Birmingham_CS.git. UK national emission inventory is

503 available at https://naei.beis.gov.uk/.

504

## Author Contribution

Jianghao Li prepared the manuscript with contributions from all authors. Alastair C. Lewis helped with modelling scenarios and revised the manuscript. Jim R. Hopkins contributed to measurement of chemical species. Stephen J. Andrews contributed to scientific discussion on findings of this work. Tim Murrells, Neil Passant and Ben Richmond contributed to the data of national emission inventory data and revision on NAEI methodology. Siqi Hou, William J. Bloss, Roy M. Harrison, and Zongbo Shi provided measurements of atmospheric pollutants used in this study, along with critical discussion on revising the manuscript.

513

## Competing interests

The authors declare that they have no conflict of interest.

516

523

## References

Abernethy, S., O'Connor, F., Jones, C., and Jackson, R.: Methane removal and the proportional reductions in surface temperature and ozone, Philosophical Transactions of the Royal Society A, 379, 20210104, 10.1098/rsta.2021.0104, 2021.

Calvert, J. G., Orlando, J. J., Stockwell, W. R., and Wallington, T. J.: The mechanisms of reactions influencing atmospheric ozone, Oxford University Press, USA, 2015.

Chen, T., Xue, L., Zheng, P., Zhang, Y., Liu, Y., Sun, J., Han, G., Li, H., Zhang, X., and Li, Y.: Volatile organic compounds and ozone air pollution in an oil production region in northern China, Atmospheric Chemistry and Physics, 20, 7069-7086, 10.5194/acp-20-7069-2020, 2020.

Cliff, S. J., Lewis, A. C., Shaw, M. D., Lee, J. D., Flynn, M., Andrews, S. J., Hopkins, J. R., Purvis,

R. M., and Yeoman, A. M.: Unreported VOC emissions from road transport including from electric vehicles, Environmental Science & Technology, 10.1021/acs.est.3c00845, 2023.

Coggon, M. M., Gkatzelis, G. I., McDonald, B. C., Gilman, J. B., Schwantes, R. H., Abuhassan, N., Aikin, K. C., Arend, M. F., Berkoff, T. A., Brown, S. S., Campos, T. L., Dickerson, R. R., Gronoff, G., Hurley, J. F., Isaacman-VanWertz, G., Koss, A. R., Li, M., McKeen, S. A., Moshary, F., Peischl, J., Pospisilova, V., Ren, X., Wilson, A., Wu, Y., Trainer, M., and Warneke, C.: Volatile chemical product emissions enhance ozone and modulate urban chemistry, Proc Natl Acad Sci U S A, 118, 10.1073/pnas.2026653118, 2021.

de Foy, B., Brune, W. H., and Schauer, J. J.: Changes in ozone photochemical regime in Fresno, California from 1994 to 2018 deduced from changes in the weekend effect, Environmental Pollution, 263, 114380, 10.1016/j.envpol.2020.114380, 2020.

Department for Environment, Food & Rural Affairs. An annual update of data on concentrations of major air pollutants in the UK: https://www.gov.uk/government/statistical-data-sets/env02-air-quality-statistics, last access: 07 September 2023.

Diaz, F. M., Khan, M. A. H., Shallcross, B. M., Shallcross, E. D., Vogt, U., and Shallcross, D. E.: Ozone trends in the United Kingdom over the last 30 years, Atmosphere, 11, 534, 10.3390/atmos11050534, 2020.

Edwards, P. M., Brown, S. S., Roberts, J. M., Ahmadov, R., Banta, R. M., deGouw, J. A., Dube, W. P., Field, R. A., Flynn, J. H., Gilman, J. B., Graus, M., Helmig, D., Koss, A., Langford, A. O., Lefer, B. L., Lerner, B. M., Li, R., Li, S. M., McKeen, S. A., Murphy, S. M., Parrish, D. D., Senff, C. J., Soltis, J., Stutz, J., Sweeney, C., Thompson, C. R., Trainer, M. K., Tsai, C., Veres, P. R., Washenfelder, R. A., Warneke, C., Wild, R. J., Young, C. J., Yuan, B., and Zamora, R.: High winter ozone pollution from carbonyl photolysis in an oil and gas basin, Nature, 514, 351-354, 10.1038/nature13767, 2014.

European Environment Agency.: EMEP/EEA air pollutant emission inventory guidebook 2016, 2016. https://www.eea.europa.eu/publications/emep-eea-guidebook-2016, last access 07 September 2023.

Finch, D. P. and Palmer, P. I.: Increasing ambient surface ozone levels over the UK accompanied by fewer extreme events, Atmospheric environment, 237, 117627, 10.1016/j.atmosenv.2020.117627, 2020.

Gaudel, A., Cooper, O. R., Chang, K.-L., Bourgeois, I., Ziemke, J. R., Strode, S. A., Oman, L. D., Sellitto, P., Nédélec, P., Blot, R., Thouret, V., and Granier, C.: Aircraft observations since the 1990s reveal increases of tropospheric ozone at multiple locations across the Northern Hemisphere, Science Advances, 6, eaba8272, doi:10.1126/sciadv.aba8272, 2020.

Gkatzelis, G. I., Coggon, M. M., McDonald, B. C., Peischl, J., Aikin, K. C., Gilman, J. B., Trainer, M., and Warneke, C.: Identifying volatile chemical product tracer compounds in US cities, Environmental Science & Technology, 55, 188-199, 10.1021/acs.est.0c05467, 2021.

Gouldsbrough, L., Hossaini, R., Eastoe, E., and Young, P. J.: A temperature dependent extreme value analysis of UK surface ozone, 1980–2019, Atmospheric Environment, 273, 118975,

573    10.1016/j.atmosenv.2022.118975, 2022.

Gouldsbrough, L., Hossaini, R., Eastoe, E., Young, P. J., and Vieno, M.: A machine learning approach to downscale EMEP4UK: analysis of UK ozone variability and trends, Atmospheric Chemistry and Physics, 24, 3163-3196, 10.5194/acp-24-3163-2024, 2024.

He, Z., Wang, X., Ling, Z., Zhao, J., Guo, H., Shao, M., and Wang, Z.: Contributions of different anthropogenic volatile organic compound sources to ozone formation at a receptor site in the Pearl River Delta region and its policy implications, Atmospheric Chemistry and Physics, 19, 8801-8816, 10.5194/acp-19-8801-2019, 2019.

Hertig, E., Russo, A., and Trigo, R. M.: Heat and ozone pollution waves in central and south Europe—characteristics, weather types, and association with mortality, Atmosphere, 11, 1271, 10.3390/atmos11121271, 2020.

Ivatt, P. D., Evans, M. J., and Lewis, A. C.: Suppression of surface ozone by an aerosol-inhibited photochemical ozone regime, Nature Geoscience, 15, 536-540, 10.1038/s41561-022-00972-9，2022.

Jenkin, M., Saunders, S., Wagner, V., and Pilling, M.: Protocol for the development of the Master Chemical Mechanism, MCM v3 (Part B): tropospheric degradation of aromatic volatile organic compounds, Atmospheric Chemistry and Physics, 3, 181-193, 10.5194/acp-3-181-2003, 2003.

Kang, M., Hu, J., Zhang, H., and Ying, Q.: Evaluation of a highly condensed SAPRC chemical mechanism and two emission inventories for ozone source apportionment and emission control strategy assessments in China, Science of The Total Environment, 813, 151922, 10.1016/j.scitotenv.2021.151922, 2022.

Kumar, P., Kuttippurath, J., von der Gathen, P., Petropavlovskikh, I., Johnson, B., McClure-Begley, A., Cristofanelli, P., Bonasoni, P., Barlasina, M. E., and Sanchez, R.: The Increasing Surface Ozone and Tropospheric Ozone in Antarctica and Their Possible Drivers, Environmental Science & Technology, 55, 8542-8553, 10.1021/acs.est.0c08491, 2021.

Lee, J. D., Drysdale, W. S., Finch, D. P., Wilde, S. E., and Palmer, P. I.: UK surface $NO_2$ levels dropped by 42% during the COVID-19 lockdown: impact on surface $O_3$, Atmospheric Chemistry and Physics, 20, 15743-15759, 10.5194/acp-20-15743-2020, 2020.

Lefohn, A. S., Malley, C. S., Smith, L., Wells, B., Hazucha, M., Simon, H., Naik, V., Mills, G., Schultz, M. G., Paoletti, E., De Marco, A., Xu, X., Zhang, L., Wang, T., Neufeld, H. S., Musselman, R. C., Tarasick, D., Brauer, M., Feng, Z., Tang, H., Kobayashi, K., Sicard, P., Solberg, S., and Gerosa, G.: Tropospheric ozone assessment report: Global ozone metrics for climate change, human health, and crop/ecosystem research, Elementa: Science of the Anthropocene, 6, 10.1525/elementa.279, 2018.

Lewis, A. C., Allan, J. D., Carruthers, D., Carslaw, D. C., Fuller, G. W., Harrison, R. M., Heal, M. R., Nemitz, E., Reeves, C., Williams, M., Fowler, D., Marner, B. B., Williams, A., Carslaw, N., Moller, S., Maggs, R., Murrells, T., Quincey, P., and Willis, P.: Ozone in the UK: Recent Trends and Future Projections. Air Quality Expert Group. https://uk-air.defra.gov.uk/library/reports.php?report_id=1064, 2021, last assess: 27 March 2024.

Lewis, A. C., Hopkins, J. R., Carslaw, D. C., Hamilton, J. F., Nelson, B. S., Stewart, G., Dernie, J., Passant, N., and Murrells, T.: An increasing role for solvent emissions and implications for future measurements of volatile organic compounds, Philosophical Transactions of the Royal Society A, 378, 20190328, 10.1098/rsta.2019.0328, 2020.

Li, J., Yu, Z., Du, Z., Ji, Y., and Liu, C.: Standoff chemical detection using laser absorption spectroscopy: a review, Remote Sensing, 12, 2771, 10.3390/rs12172771, 2020.

Liu, Q., Gao, Y., Huang, W., Ling, Z., Wang, Z., and Wang, X.: Carbonyl compounds in the atmosphere: A review of abundance, source and their contributions to $O_3$ and SOA formation, Atmospheric Research, 106184, 10.1016/j.atmosres.2022.106184, 2022a.

Liu, T., Hong, Y., Li, M., Xu, L., Chen, J., Bian, Y., Yang, C., Dan, Y., Zhang, Y., and Xue, L.: Atmospheric oxidation capacity and ozone pollution mechanism in a coastal city of southeastern China: analysis of a typical photochemical episode by an observation-based model, Atmospheric Chemistry and Physics, 22, 2173-2190, 10.5194/acp-22-2173-2022, 2022b.

Liu, Z., Doherty, R. M., Wild, O., O'connor, F. M., and Turnock, S. T.: Tropospheric ozone changes and ozone sensitivity from the present day to the future under shared socio-economic pathways, Atmospheric Chemistry and Physics, 22, 1209-1227, 10.5194/acp-22-1209-2022, 2022.

McDonald, B. C., De Gouw, J. A., Gilman, J. B., Jathar, S. H., Akherati, A., Cappa, C. D., Jimenez, J. L., Lee-Taylor, J., Hayes, P. L., and McKeen, S. A.: Volatile chemical products emerging as largest petrochemical source of urban organic emissions, Science, 359, 760-764, 10.1126/science.aaq0524, 2018.

Monks, P. S., Allan, J. D., Carruthers, D., Carslaw, D. C., Fuller, G. W., Harrison, R. M., Heal, M. R., Lewis, A. C., Nemitz, E., Reeves, C., Williams, M., Fowler, D., Marner, B. B., Williams, A., Moller, S., Maggs, R., Murrells, T., Quincey, P., and Willis, P.: Non-methane Volatile Organic Compounds in the UK, Air Quality Group. https://uk-air.defra.gov.uk/library/reports.php?report_id=10032020, 2020, last access: 07 September 2023.

National Atmospheric Emissions Inventory.: UK Informative Inventory Report (1990 to 2019), 2021. https://naei.beis.gov.uk/reports/reports?report_id=1016, last access: 07 September 2023.

Nelson, B. S., Stewart, G. J., Drysdale, W. S., Newland, M. J., Vaughan, A. R., Dunmore, R. E., Edwards, P. M., Lewis, A. C., Hamilton, J. F., and Acton, W. J.: In situ ozone production is highly sensitive to volatile organic compounds in Delhi, India, Atmospheric Chemistry and Physics, 21, 13609-13630, 10.5194/acp-21-13609-2021, 2021.

Qin, M., Murphy, B. N., Isaacs, K. K., McDonald, B. C., Lu, Q., McKeen, S. A., Koval, L., Robinson, A. L., Efstathiou, C., and Allen, C.: Criteria pollutant impacts of volatile chemical products informed by near-field modelling, Nature sustainability, 4, 129-137, 10.1038/s41893-020-00614-1, 2021.

Saunders, S. M., Jenkin, M. E., Derwent, R., and Pilling, M.: Protocol for the development of the Master Chemical Mechanism, MCM v3 (Part A): tropospheric degradation of non-aromatic

volatile organic compounds, Atmospheric Chemistry and Physics, 3, 161-180, 10.5194/acp-3-161-2003, 2003.

Schroeder, J. R., Crawford, J. H., Ahn, J.-Y., Chang, L., Fried, A., Walega, J., Weinheimer, A., Montzka, D. D., Hall, S. R., and Ullmann, K.: Observation-based modeling of ozone chemistry in the Seoul metropolitan area during the Korea-United States Air Quality Study (KORUS-AQ), Elementa: Science of the Anthropocene, 8, 3, 10.1525/elementa.400, 2020.

Seinfeld, J. H. and Pandis, S. N.: Atmospheric chemistry and physics: from air pollution to climate change, John Wiley & Sons, 2016.

Sicard, P.: Ground-level ozone over time: an observation-based global overview, Current Opinion in Environmental Science & Health, 19, 100226, 10.1016/j.eti.2022.102809, 2021.

Sicard, P., Paoletti, E., Agathokleous, E., Araminienė, V., Proietti, C., Coulibaly, F., and De Marco, A.: Ozone weekend effect in cities: Deep insights for urban air pollution control, Environmental Research, 191, 110193, 10.1016/j.envres.2020.110193, 2020.

Tarasick, D., Galbally, I. E., Cooper, O. R., Schultz, M. G., Ancellet, G., Leblanc, T., Wallington, T. J., Ziemke, J., Liu, X., and Steinbacher, M.: Tropospheric Ozone Assessment Report: Tropospheric ozone from 1877 to 2016, observed levels, trends and uncertainties, Elementa: Science of the Anthropocene, 7, 39, 10.1525/elementa.376, 2019.

Wang, S., Yuan, B., Wu, C., Wang, C., Li, T., He, X., Huangfu, Y., Qi, J., Li, X.-B., and Sha, Q. e.: Oxygenated volatile organic compounds (VOCs) as significant but varied contributors to VOC emissions from vehicles, Atmospheric Chemistry and Physics, 22, 9703-9720, 10.5194/acp-22-9703-2022, 2022.

Wang, Y., Guo, H., Zou, S., Lyu, X., Ling, Z., Cheng, H., and Zeren, Y.: Surface $O_3$ photochemistry over the South China Sea: Application of a near-explicit chemical mechanism box model, Environmental Pollution, 234, 155-166, 10.1016/j.envpol.2017.11.001, 2018.

Warburton, T., Grange, S. K., Hopkins, J. R., Andrews, S. J., Lewis, A. C., Owen, N., Jordan, C., Adamson, G., and Xia, B.: The impact of plug-in fragrance diffusers on residential indoor VOC concentrations, Environmental Science: Processes & Impacts, 25, 805-817, 10.1039/D2EM00444E, 2023.

Winkler, S., Anderson, J., Garza, L., Ruona, W., Vogt, R., and Wallington, T.: Vehicle criteria pollutant (PM, $NO_x$, CO, HCs) emissions: how low should we go?, Npj Climate and atmospheric science, 1, 26, 10.1038/s41612-018-0037-5, 2018.

Wolfe, G. M., Marvin, M. R., Roberts, S. J., Travis, K. R., and Liao, J.: The framework for 0-D atmospheric modeling (F0AM) v3. 1, Geoscientific Model Development, 9, 3309-3319, 10.5194/gmd-9-3309-2016, 2016.

Wu, R. and Xie, S.: Spatial Distribution of Ozone Formation in China Derived from Emissions of Speciated Volatile Organic Compounds, Environmental Science & Technology, 51, 2574-2583, 10.1021/acs.est.6b03634, 2017.

Yeoman, A. M. and Lewis, A. C.: Global emissions of VOCs from compressed aerosol products, Elementa: Science of the Anthropocene, 9, 00177, 10.1525/elementa.2020.20.00177, 2021.

690     Zulkifli, M. F. H., Hawari, N. S. S. L., Latif, M. T., Abd Hamid, H. H., Mohtar, A. A. A., Idris, W.

691         M. R. W., Mustaffa, N. I. H., and Juneng, L.: Volatile organic compounds and their contribution

692         to ground-level ozone formation in a tropical urban environment, Chemosphere, 302, 134852,

693         10.1016/j.chemosphere.2022.134852, 2022.

694